AIAA JOURNAL
Vol. 39, No. 9, September 2001

Numerical Assessment of Error Estimators for Euler Equations

X. D. Zhang*
Centre de Recherche en Calcul Appliqué, Montréal, Québec H3X 2H9, Canada
and
D. Pelletier,† J.-Y. Trépanier,‡ and R. Camarero§
École Polytechnique de Montréal, Montréal, Québec H3C 3A7, Canada

Grid convergence studies are conducted to assess four error estimators for their asymptotic behavior: explicit residual, solution reconstruction, Richardson extrapolation, and solution of the error equations. Their accuracy, reliability, and efficitivity to predict the true error are verified on the quasi-one-dimensional Euler equations solved by a second-order accurate finite volume method.

Nomenclature

$\mathcal{D}$	=	cross-sectional area function
E	=	specific total energy
e	=	solution error
f	=	flux function
h	=	grid size
$\mathcal{L}$	=	linear differential operator
p	=	pressure
R	=	ratio of grid refinement
r	=	descritization residual of equation
s	=	source term of equation
u	=	solution variables
v	=	fluid velocity
x	=	coordinate
θ	=	effectivity index
ρ	=	fluid density
Ω	=	computational domain

Subscripts

eeq	=	solution of error equations
h	=	numerical approximation
i	=	cell center value of variable
K	=	grid element or cell
L	=	left state of variable
R	=	right state of variable
rect	=	solution reconstruction error estimator
Rich	=	Richardson extrapolation error estimator
rsd	=	residual error estimator
t	=	derivative in time
W	=	functional space
x	=	derivative in space

Superscripts

n	=	number of time steps
α	=	convergence rate

Introduction

THE rapidly increasing power of computers enables very accurate approximations of solutions to partial differential equations. For complex problems, highly accurate numerical solutions of partial differential equations can be achieved using locally adaptive grids. The generation of such adapted grids is usually guided by a proper error estimator or indicator. Analyses of the error and its estimate abound for elliptic equations solved with finite element methods. However, for nonlinear hyperbolic problems, the theoretical foundation of a posteriori and a priori error analysis is far from satisfactory. The difficulties in estimating the errors and its control for hyperbolic equations have received more attentions only recently, despite its importance in practical applications. Some efforts on error estimates for hyperbolic equations can be found in Refs. 1–4.

Because of the lack of sound theoretical analyses, many practitioners simply choose one error indicator to guide mesh adaptation. Such indicators are usually based on the local gradient of a key variable,[5,6] such as fluid density, based on the idea that the error occurs when the variable of interest varies sharply. A more reasonable error indicator is based on the residual of the discretized equation[2,3] because it is a more reliable indication of how accurately the differential equation has been solved. Another method is to use two different levels of approximation (solution reconstruction),[7,8] which is suitable to estimate interpolation error. Another approach is to use solutions on two or three different levels of grid refinement to perform Richardson extrapolation to estimate solution error.[9] Finally, one can solve error equations with residuals as the right-hand side to provide the solution error[4,10] that account for the transport of errors. All of these error estimators except for the last one are extensions from finite element methods for elliptic equations. For hyperbolic equations, several of these techniques are questionable.

One important issue for any a posteriori error estimator or indicator is its ability to predict the discretization error of the numerical method. At the least, one requires that the estimated error and the true error should have the same asymptotic convergence rate when the mesh is refined. For hyperbolic problems, very little theoretical analyses can be found about convergence rate and asymptotic behaviors of the mentioned error estimations because of the lack of mathematical foundations. Because these properties are so important in the control and minimization of the discretization error, it is worthwhile to conduct numerical investigations or verifications for test problems. The motivation of this paper is to perform careful studies of various error estimators through numerical experiments. The main purpose of this paper is to assess existing error estimators in various norms for their accuracy and reliability.

Different Error Estimations

Global solution error is generally predicted by a priori error estimates for a given numerical method. It establishes the convergence of the method when the grid size tends to zero, a basic requirement for any numerical methods. The a priori error estimate may be expressed as

$$\|u - u_h\|_{W,\Omega} = \mathcal{O}(h^{\alpha}) \qquad \text{with} \qquad h = \max_{K \in \mathcal{P}_h}(h_K) \tag{1}$$

Presented as Paper 2000-1001 at the AIAA 38th Aerospace Sciences Meeting, Reno, NV, 10–13 January 2000; received 19 February 2000; revision received 20 March 2001; accepted for publication 5 April 2001.

*Research Professional; xzhang@virtualprototypes.ca. Member AIAA.
†Professor, Département de Génie Mécanique; dp@cerca.umontreal.ca. Associate Fellow AIAA.
‡Associate Professor, Département de Génie Mécanique; jyves@cerca.umontreal.ca. Member AIAA.
§Professor, Département de Génie Mécanique; ricardo@cerca.umontreal.ca. Member AIAA.

where u is the exact solution, u_h is an approximate solution, $\|\cdot\|_{W,\Omega}$ is a proper norm over the whole domain Ω in a Sobolev space W, $\mathcal{P}_h$ is the mesh partition established over $\bar{\Omega}$, and h_K represents the size of the cell $K \in \mathcal{P}_h$. The superscript $\alpha > 0$ represents the convergence rate for the numerical method. For approximations of elliptic equations using finite element methods, this type of error estimation with $W = H^1(\Omega)$ may be found in Ref. 11. For approximations of hyperbolic equations using finite volume methods, similar results with L_2 norm were given in Ref. 12. It is evident that the rate of convergence depends on both the problem and the numerical method. It is also strongly dependent on the norm used to measure the error.

The exact error is usually not available for most problems of interest. To be able to control the true error globally, one controls the estimated error instead. However, the purpose of using adaptive technique to control the estimated error is to allow us ultimately to control the true error. This requires that the estimated error must have a behavior similar to that of the true error. The effectivity index defined by

$$\theta = \|e\|/\|u - u_h\|$$

for an estimated error $\|e\|$ is a measure for its reliability and effectivity. The property of asymptotic exactness ($\theta \to 1$ when $h \to 0$) is not essential for grid adaptation. A reasonable constant difference should be good enough to guide the adaptation and control the true error as well. Lack of proper asymptotic behavior ($\theta \to 0$ or $\theta \to \infty$ when $h \to 0$) may mislead the grid adaptation and the error control.

Variable Derivatives and Residuals

An early error estimator that is still commonly used is based on local derivatives (gradient, divergence, or curl) of a key variable.[5,6] The idea behind this strategy is that errors occur in regions of rapid changes in the solution. To avoid unbounded derivatives across discontinuities, the estimated error using derivatives is usually multiplied by a power of local length of the grid cell.[8] This type of error indicator used for mesh adaptation works well for some cases, but cannot be viewed as a rigorous error estimator because of its lack of theoretical foundation. Also, use of large gradients as a grid refinement indicator can be misleading. For instance, a uniform shear flow can exhibit an arbitrary large velocity gradient and yet can be solved exactly with a single linear finite element.

Note that, for steady state problem of the Euler equation, the derivative of variable $\mathcal{D}\rho u$ is simply the residual of the continuity equation. However, the residual is better at measuring how well the differential equation has been satisfied than at measuring the solution error itself.

Following Babuška and Rheinboldt,[13] some efforts have been focused on explicit residual-type error estimators.[14,15] Consider the partial differential equation

$$\mathcal{L}u = f \tag{2}$$

over a given domain Ω for a linear differential operator $\mathcal{L}$. Let u_h be the numerical approximation to the exact solution u and $r = \mathcal{L}u_h - f$ the corresponding residual. The equation for the error $e = u - u_h$ can be written as

$$\mathcal{L}e = r \tag{3}$$

and one has

$$\|e\|_{(1)} \le c\|r\|_{(2)} \tag{4}$$

with suitable norms $\|\cdot\|_{(1)}$ and $\|\cdot\|_{(2)}$ and a constant c. For nonlinear equations, a constant c may not exist making the analysis more difficult. The L_2 norm is the traditional natural choice. However, as demonstrated in Refs. 14 and 15, $\|r\|_{L_2} = \mathcal{O}(h^{-1/2})$, so that it is uncontrollable for one-dimensional hyperbolic problems in the presence of shocks. To control the error, weak measures[14] of the residual have been used over each element K. For example,

$$e_{L_2} = \|hr\|_{L_2(K)}, \qquad e_{H^{-1}} = \|r\|_{H^{-1}(K)} \tag{5}$$

have been proposed in Ref. 14. Because the norm $\|\cdot\|_{H^{-1}(K)}$ is not computable in practice, an approximation[14,15] was used to evaluate its value in each element K:

$$\|r\|_{H^{-1}(K)} \approx \max_i \frac{\left|\int_K r\phi_i \, \mathrm{d}x\right|}{\|\phi_i\|_{H_1(K)}}$$

where ϕ_i, $i = 1, 2, \ldots, n_i$, are some properly chosen functions in $H_0^1(K)$. With this approximation, the two weak norms given in Eq. (5) are typically equivalent.[16] With these error estimations as refinement indicators, impressive results have been reported for compressible Euler equations.[3,15,16]

Note that the first measure in Eq. (5) has the same form as that of the error estimator of Babuška and Rheinboldt,[13] except for a multiplicative constant. Although the error estimator of Babuška and Rheinboldt is asymptotically exact[13] for finite element solutions of second-order elliptic equations, it is not clear that this property also holds for hyperbolic equations. However, the work of Süli and Houston[17] shows that the global error measured in a weak norm in H^1 is bounded from above by the residual as

$$\|u - u_h\|_{H^{-1}(\Omega)} \le C\|hr\|_{L^2(\Omega)} \tag{6}$$

In this paper, the residual-based error estimator to be verified is denoted by

$$\mathrm{err}_{\mathrm{rsd}} := r \tag{7}$$

with a proper norm $\|\cdot\|$. The effect of the multiplicative constant is neglected. For example, the L_1 and L_2 norms are calculated as follows:

$$\|\mathrm{err}_{\mathrm{rsd}}\|_{L_1} = \|r\|_{L_1(K)} \approx h_K|r|_K$$

$$\|\mathrm{err}_{\mathrm{rsd}}\|_{L_2} = \|r\|_{L_2(K)} \approx h_K^{\frac{1}{2}}|r|_K \tag{8}$$

where $|r|_K$ is the absolute value of residual at the central point of K. The central value of $r(u_h)$ is computed by a least-square approximation.

Solution Reconstruction

Another type of error estimator is based on solution reconstruction.[7,8,18] The idea is as follows: One expects to estimate the solution error $e = u - u_h$ without knowing the exact solution u. The order of the scheme generally represents the order of interpolation for u_h. A higher-order reconstruction of u based on u_h should yield a better approximation to u. Thus, the difference between the reconstruction and the approximate solution can be used as an error estimator.

For piecewise linear approximations of u_h (second-order scheme), the error is approximated as the departure from the quadratic, which results in

$$e_K = \left(a_1x^2 + a_2xh + a_3h^2\right)\frac{\mathrm{d}^2u_h}{\mathrm{d}x^2}$$

where a_1, a_2, and a_3 are constants depending on the linear approximation, limiters, etc. For example, if the piecewise linear approximation is used between two node values (such as in finite element methods), the quadratic departure is

$$(e_K)_1 = \frac{1}{2}x(h - x)\frac{\mathrm{d}^2u_h}{\mathrm{d}x^2}$$

If the piecewise linear approximation is extended from the cell-centered value to its endpoints (such as in most finite volume methods without limiter), the quadratic departure in the control volume is

$$(e_K)_2 = \begin{cases} \dfrac{1}{2}x^2\dfrac{\mathrm{d}^2u_h}{\mathrm{d}x^2}(0), & 0 \le x < h/2 \\ \dfrac{1}{2}(x-h)^2\dfrac{\mathrm{d}^2u_h}{\mathrm{d}x^2}(h), & h/2 \le x \le h \end{cases}$$

For simplicity, here the origin of x is placed at one end point of K for one-dimensional problems. It is clearly shown that different approximations end up with different constants. It is very difficult to define those constants when limiters are used. In the following, the effects of the constants will be neglected.

This type of error estimation is an analog of the approximation error of finite element methods. Only the local variation of the variables has been used. It has been demonstrated to be effective for elliptic equations. For hyperbolic cases, its effectivity has not been proven especially across discontinuities. Furthermore, it does not account for the transport of the error.

In this paper, the solution reconstruction based error estimator to be verified is denoted by

$$\mathrm{err}_{\mathrm{rect}} := e_K \tag{9}$$

with a proper norm $\|\cdot\|$. More specifically, the L_1 and L_2 norms are approximated by neglecting the effect of the multiplicative constant:

$$\|\mathrm{err}_{\mathrm{rect}}\|_{L_1} = \|e_K\|_{L_1(K)} \approx h_K^3 \left|\frac{\mathrm{d}^2 u_h}{\mathrm{d}x^2}\right|_K$$

$$\|\mathrm{err}_{\mathrm{rect}}\|_{L_2} = \|e_K\|_{L_2(K)} \approx h_K^{\frac{5}{2}} \left|\frac{\mathrm{d}^2 u_h}{\mathrm{d}x^2}\right|_K \tag{10}$$

where the second derivatives are calculated using a least-square approximation. Tests using a central difference provide almost the same results. The reason to use least-square approximation is that it can easily be extended to two- and three-dimensional unstructured meshes.

Note that in Ref. 7 the norm used to estimate the local error is the root mean square value of the e_K, that is,

$$\|\mathrm{err}_{\mathrm{rect}}\|_{\mathrm{rms}} = \left\{\int_0^h \frac{(e_K)_1^2}{h}\mathrm{d}x\right\}^{\frac{1}{2}} = h_K^{\frac{1}{2}}\|(e_K)_1\|_{L_2(K)}$$

$$= \frac{h_K^2}{\sqrt{120}}\left|\frac{\mathrm{d}^2 u_h}{\mathrm{d}x^2}\right|_K \tag{11}$$

where the constant $1/\sqrt{120}$ results from the integration of the polynomial in x and has been approximated by $\frac{1}{11}$ in Ref. 7. However, the convergence rate of the norm of root mean square error is actually a half-order higher than that of the L_2 norm.

Richardson Extrapolation

Richardson extrapolation is based on a Taylor series expansion of the discrete solution. The idea behind this approach is to combine two discrete solutions on two different grids (one finer than the other) to obtain the leading terms in the expansion of the error. This approach has been used by Roache to compute the grid convergence index (GCI) (for more details, see Refs. 9 and 19).

One of the important factors in this approach is to determine the convergence rate of the numerical method. This is generally not easy for upwind schemes especially when limiters are used.[20] Roache[9,19] has proposed to use three grids when the exact solution is not known. Assume that u_{h_1}, u_{h_2}, and u_{h_3} are three solutions on three different grids with refinement ratio of $R = h_2/h_1 = h_3/h_2 > 1$, then the estimated convergence rate is given by

$$\alpha = \ln\left(\frac{\|u_{h_3} - u_{h_2}\|}{\|u_{h_2} - u_{h_1}\|}\right) \Big/ \ln(R) \tag{12}$$

where $\|\cdot\|$ represents a norm used in the error estimation. If one knows the closed-form solution u, two discrete solutions on two different grids will be sufficient to determine α by

$$\alpha = \ln\left(\frac{\|u - u_{h_2}\|}{\|u - u_{h_1}\|}\right) \Big/ \ln(R) \tag{13}$$

The Richardson extrapolation starts from a Taylor series representation of u_h

$$u_h = u + a_1 h + a_2 h^2 + a_3 h^3 + \cdots$$

where a_i are grid-independent coefficients in the asymptotic region. For an α-th order scheme (if α is an integer, then $a_i = 0$ for $i < \alpha$), the exact solution u can be approximated by two solutions on different grids with h_1 and h_2 ($R = h_2/h_1$) as

$$u = u_{h_1} + \frac{u_{h_1} - u_{h_2}}{R^\alpha - 1}$$

Consequently, the Richardson error estimate on a coarse grid is $u_{h_2} - u$ can be derived, and it is denoted by

$$\mathrm{err}_{\mathrm{Rich}} := [R^\alpha/(R^\alpha - 1)]\left(u_{h_2} - u_{h_1}\right) \tag{14}$$

For L_1 and L_2 norms, the preceding error estimations are given by

$$\|\mathrm{err}_{\mathrm{Rich}}\|_{L_1} = \frac{R^{\alpha_{L1}}}{|R^{\alpha_{L1}} - 1|}\left\|u_{h_2} - u_{h_1}\right\|_{L_1(K)}$$

$$\|\mathrm{err}_{\mathrm{Rich}}\|_{L_2} = \frac{R^{\alpha_{L2}}}{|R^{\alpha_{L2}} - 1|}\left\|u_{h_2} - u_{h_1}\right\|_{L_2(K)} \tag{15}$$

Error Equation

Finally, solving the error equation (3) with residuals as the right-hand side provides another approach,[4,10] which accounts for the wave structure of the solution and is expected to detect the nonlocal transport error. The error equations may be solved using a higher-order scheme[4] or a different mesh.[10]

In this paper, the error equations and corresponding boundary conditions for the steady-state errors are the ones given in Ref. 21, that is,

$$e_t + [A(u_h)e]_x = -r(u_h) \tag{16}$$

where $A(u_h)$ is the linearized matrix from the original Euler equations. The time-dependent term in Eq. (16) is introduced for time marching to steady state. This is a linear hyperbolic system of equations for the error vector with an extra error source given by the residual $-r(u_h)$.

Thus, the error estimator using the error equations to be verified in this paper is denoted by

$$\mathrm{err}_{\mathrm{eeq}} := e \tag{17}$$

with a proper norm $\|\cdot\|$.

Numerical Tests

The test case is the steady quasi-one-dimensional Euler equations representing compressible flow in a duct of variable cross section:

$$u_t + [f(u)]_x = s$$

in which

$$u = \mathcal{D}\begin{pmatrix}\rho\\ \rho v\\ \rho E\end{pmatrix}, \qquad f(u) = \mathcal{D}\begin{pmatrix}\rho v\\ \rho v^2 + p\\ \rho v E + vp\end{pmatrix}$$

$$s = \begin{pmatrix}0\\ p\dfrac{\partial \mathcal{D}}{\partial x}\\ 0\end{pmatrix}$$

For the quasi-one-dimensional problem, closed-form solutions can be calculated when the area function $\mathcal{D}(x)$ is known.[22]

Test cases have been conducted using two geometries defined by area functions in the interval [0, 8]. The first one is given by

$$\mathcal{D}_1(x) = \begin{cases} d_1, & 0.0 \le x \le 0.5\\ d_1 - k(x - 0.5)^2, & 0.5 < x \le 1.5\\ 2.25 - \frac{2}{3}\arctan[4(x - 2.5)], & 1.5 < x \le 3.0\\ a(x - 2) + b/(x - 2), & 3.0 < x \le 6.0\\ d_2 + d_3[1 - (x - 7)^2], & 6.0 < x \le 7.0\\ d_2 + d_3, & 7.0 < x \le 8.0 \end{cases}$$

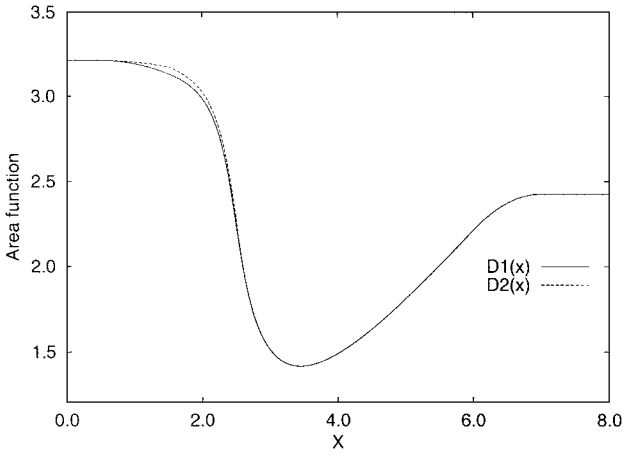

Fig. 1 Area functions for the two geometries.

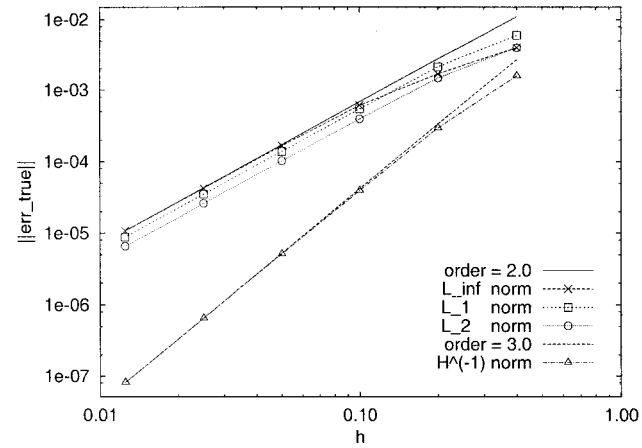

Fig. 2 Supersonic flow: true momentum error in different norms.

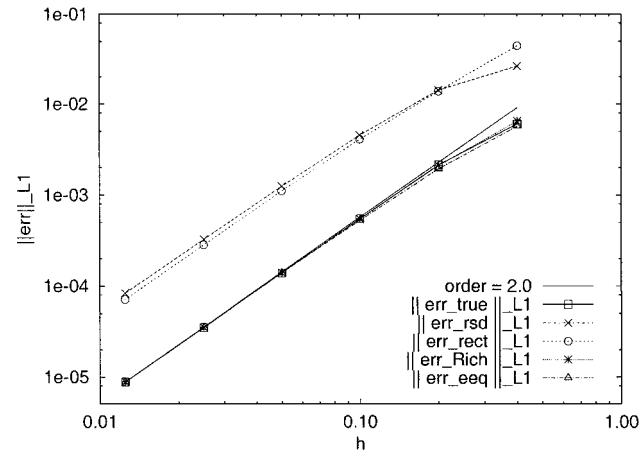

Fig. 3 Supersonic flow: estimated momentum errors in L_1 norm.

where $k=\frac{4}{51}$, $a=1.125-\frac{4}{15}-\arctan(2)/3$, $b=1.125+\frac{4}{15}-\arctan(2)/3$, $d_1=2.25+k-2\arctan(-4)/3$, $d_2=4a+b/4$, and $d_3=(a-b/16)/2$ are constants. This function is piecewise C^∞ smooth and C^1 smooth at the joining points. To reduce the effect of boundary condition treatment, the nozzle is extended at both ends by a length of constant cross-sectional duct. To check the effect of the smoothness of the geometry, a slightly modified area function from $\mathcal{D}_1(x)$ is defined as

$$\mathcal{D}_2(x)=\begin{cases} d_1, & 0.0\le x\le 0.5\\ d_1-(k+c)(x-0.5)^2, & 0.5<x\le 1.5\\ 2.25-\frac{2}{3}\arctan[4(x-2.5)]-c, & 1.5<x\le 2.5\\ a(x-2)+[b/(x-2)], & 2.5<x\le 6.0\\ d_2+d_3[1-(x-7)^2], & 6.0<x\le 7.0\\ d_2+d_3, & 7.0<x\le 8.0 \end{cases}$$

where $c=1.85-1.25(a+b)$ is another constant. The second area function is also C^1 smooth except at $x=2.5$, where it is only C^0 smooth. However, the areas at the inlet, outlet, and throat $[x=2+(b/a)^{1/2}]$ are the same for both geometries. The slight differences between these two geometries are shown in Fig. 1.

In the present work, a uniform mesh refinement study is performed starting with a mesh of 21 points. The number of points used over the interval [0,8] ranges from 21 to 641 with five meshes for supersonic and subsonic cases and from 21 to 1281 points with six meshes for the transonic case. Unless stated otherwise, results are reported for geometry $\mathcal{D}_1(x)$. The norms are defined globally on the whole interval. For example, the L_1 and L_2 norms are given by

$$\|e\|_{L_1}=\sum_K \|e\|_{L_1(K)}, \qquad \|e\|_{L_2}=\left(\sum_K \|e\|^2_{L_2(K)}\right)^{\frac{1}{2}}$$

A finite volume explicit time-marching scheme is used to solve the the Euler equations. For a uniform mesh, the time-marching procedure can be written as

$$u^{n+1}_{h,i}=u^n_{h,i}-\frac{\Delta t}{\Delta x}\left(f^n_{i+\frac{1}{2}}-f^n_{i-\frac{1}{2}}-\Delta x s^n_i\right) \tag{18}$$

The interface flux values $f^n_{i\pm 1/2}$ are computed using a modified Roe's characteristic upwind flux-difference-splitting scheme to treat the source term more accurately.[23] With these modifications, the scheme is second-order accurate for steady-state solutions over smooth flow regions (for details, see Ref. 23).

Supersonic Case

First we consider a shockless supersonic flow. The inlet condition is specified with a Mach number of $M_\infty=3.5$, and other variables are evaluated using isentropic relations. At the outflow boundary, the variables are extrapolated from the last cell.

The exact momentum error with norms of L_∞, L_1, L_2, and H^{-1} are plotted in Fig. 2 and compared with the second- and the third-order reference lines for convergence. It is evident that the H^{-1} norm of the error is of order three, whereas the others are of order two. This indicates that the accuracy of the scheme is second order when measured with both the L_1 and L_2 norms. Because the variables are smooth, the L_∞ norm is also second-order accurate. The behaviors for other variables such as density and total energy are similar and are not plotted.

The convergence rate estimated from Eq. (12) using the last three grids are $\alpha_1=1.98$ and $\alpha_2=1.97$ for the L_1 and L_2 norms, respectively. They are quite close to the expected value of $\alpha=2$. The L_1 and L_2 norms of the estimated momentum errors (i.e. the error in variable $\mathcal{D}\rho v$) using the reconstruction, Richardson extrapolation, error equation, and the error indicator using the residual for continuity equation (it is actually the residual of equation $\partial\mathcal{D}\rho v/\partial x=0$ for a steady-state problem) are compared with the true momentum error in Figs. 3 and 4. Figures 3 and 4 show that all error estimators have convergence rates very close to $\alpha=2$. Note that the weak norm of the residual defined by Eq. (5) has a convergence rate of about $\alpha=3$ because of the inclusion of the grid size h in its definition. This is consistent with the true error measure in the H^{-1} norm (shown in Fig. 2) and Eq. (6).

However, when the second geometry with area function $\mathcal{D}_2(x)$ is used, the L_2 norm of the residual error indicator behaves differently, whereas the others do not change when compared to the results obtained in the first geometry. The difference is that the L_2 norm of $\mathrm{err}_{\mathrm{rsd}}$ is half an order lower than in the earlier case, as shown in Fig. 5. This is attributed to the lower smoothness of the geometry where sharp changes of the solutions are observed. For such cases, though the error bound formula given by Süli and Houston[17] [Eq. (6)] is still valid, the effectivity index defined in Eq. (4) for the residual

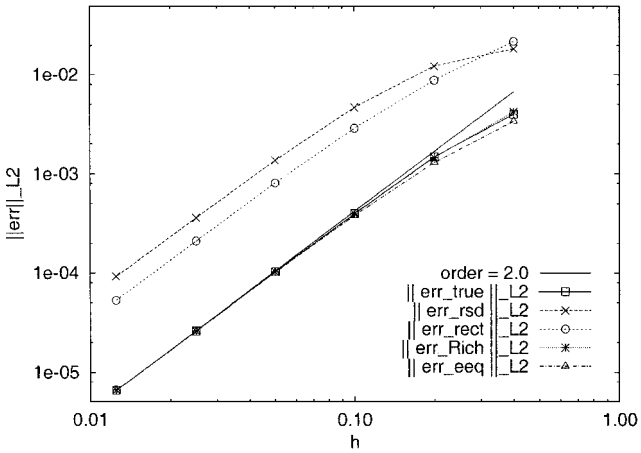

Fig. 4 Supersonic flow: estimated momentum errors in L_2 norm.

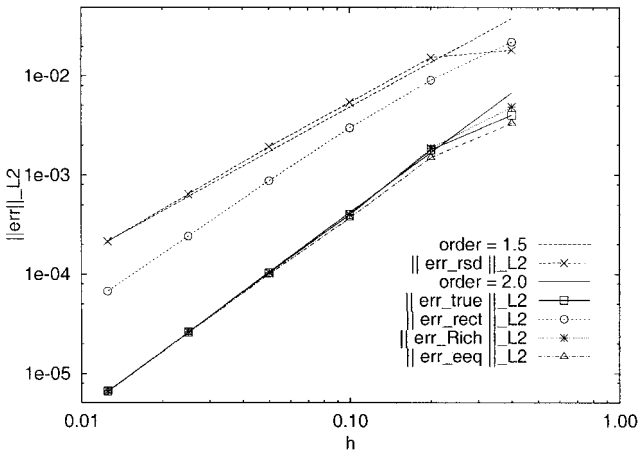

Fig. 5 Supersonic flow: estimated momentum errors in L_2 norm for nozzle $\mathcal{D}_2(x)$.

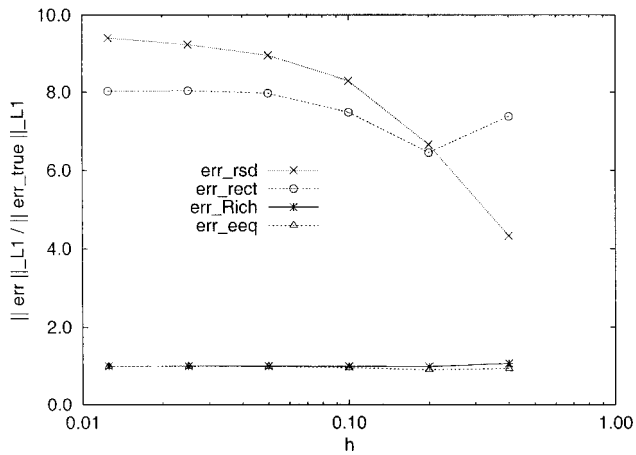

Fig. 6 Supersonic flow: effectivity index of estimators in L_1 norm.

error indicator tends to infinity. Thus, using such an error indicator (L_2 norm) to guide grid adaptation is questionable. However, the L_1 norm of the residual seems less dependent on the smoothness of the geometry and may be a more reliable error indicator. Surprisingly, the error estimator based on the error equation does not show the same departure in the L_2 norm even if the residual acts as source terms in the error equations.

The asymptotic performance of these error estimators is demonstrated in Fig. 6 by comparing their effectivity index. The error estimators based on residual and reconstruction are about 8–10 times larger in magnitude than the true error. This is because the

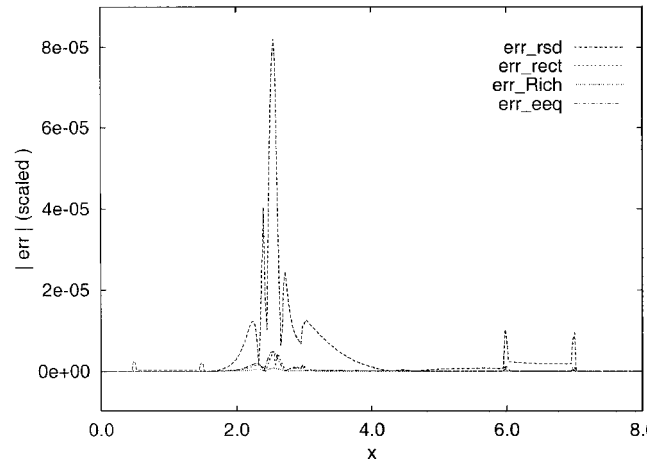

Fig. 7 Supersonic flow: error distributions.

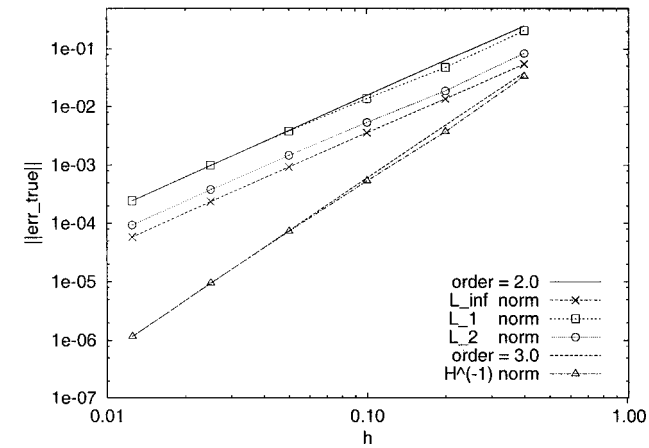

Fig. 8 Subsonic flow: true momentum error in different norms.

multiplicative constants have been neglected for estimators based on residual and reconstruction. To recover appropriate asymptotic exactness, two scaling constants $c_1 = \frac{1}{10} = 0.1$ and $c_2 = \frac{1}{8.3} = 0.12$ may be used. Such constant scaling may not be necessary and also is not practical in grid adaptation, but such scaling may be useful to check their universality when applied to different problems and to check the agreement of local error distribution. Actually, Fig. 7 shows the very good agreement of the estimated local momentum errors over the grid of 321 points when compared with the true error. The explicit residual approach is the exception.

If one compares the formulation of Peraire et al.,[7] for example, the constant is $c = 1/\sqrt{120}$ as given in Eq. (11) for the reconstruction error estimator, which is in close agreement with our scaling factor of $c_2 = 0.12$.

Although the residual error indicator may be equivalent to other estimators[24] and be very reliable for elliptic equations,[13,25] it does not behave as well for hyperbolic equations, as discussed in Refs. 4, 17, and 26. Furthermore, for hyperbolic cases the error may not be the appropriate criterion to guide mesh adaptation. Indeed, insufficient mesh resolution may manifest itself as an error far downstream due to the convection of errors. In such a case, one must refine the mesh at the upwind source of the error.

Subsonic Case

The second test case is an isentropic subsonic nozzle. At the inlet, pressure is extrapolated from the first cell value, whereas other variables are computed using isentropic flow condition with unit total pressure and temperature. At the outflow boundary, the normalized back pressure is set to $p = 0.93$. The velocity and the temperature are extrapolated from the last cell.

The true momentum errors measured in L_∞, L_1, L_2, and H^{-1} norms are plotted in Fig. 8. The H^{-1} norm converges with third-order accuracy, whereas others exhibit a converge rate of two.

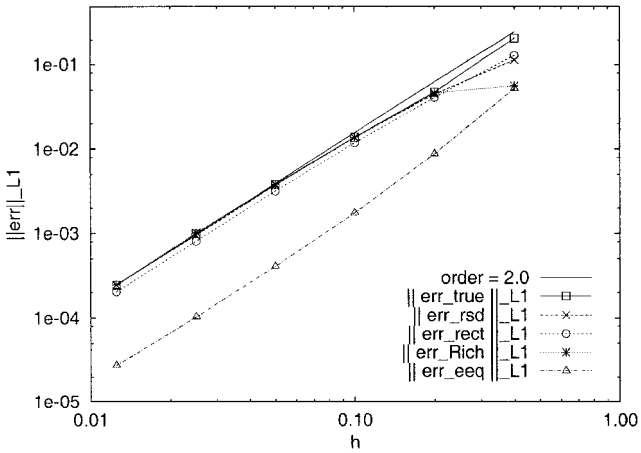

Fig. 9 Subsonic flow: estimated momentum errors in L_1 norm.

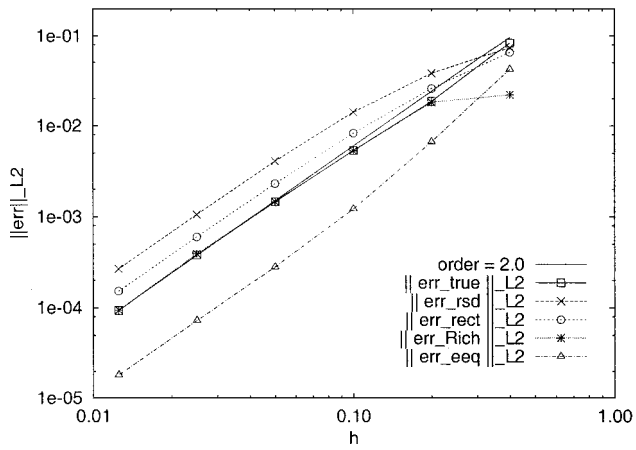

Fig. 10 Subsonic flow: estimated momentum errors in L_2 norm.

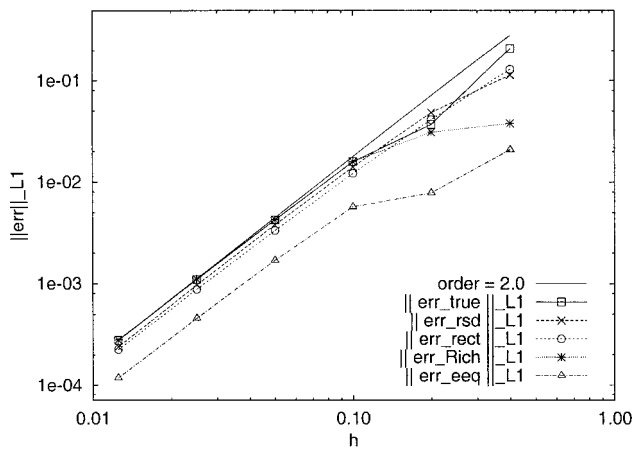

Fig. 11 Subsonic flow: estimated momentum errors in L_1 for nozzle $\mathcal{D}_2(x)$.

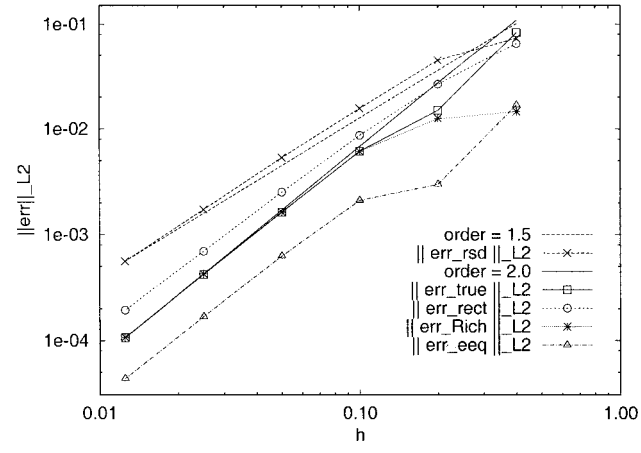

Fig. 12 Subsonic flow: estimated momentum errors in L_2 for nozzle $\mathcal{D}_2(x)$.

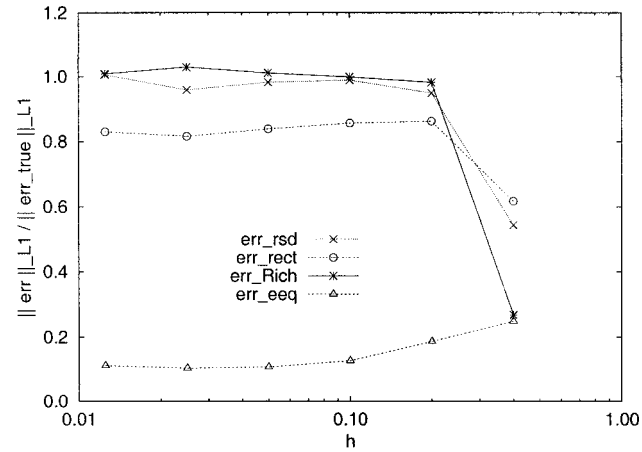

Fig. 13 Subsonic flow: effectivity index of estimators in L_1 norm.

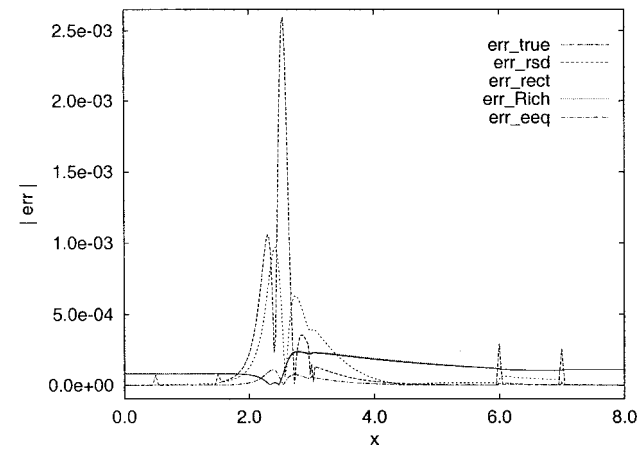

Fig. 14 Subsonic flow: error distributions.

Figures 9 and 10 present a comparison of the estimated errors with L_1 and L_2 norms using the four error estimators discussed earlier.

The convergence rate estimated from Eq. (12) using the last three grids are $\alpha_1 = 1.91$ and $\alpha_2 = 1.91$ for the L_1 and L_2 norms, respectively. They are slightly lower than in the supersonic case. Again, the same behavior using geometry $\mathcal{D}_2(x)$ is observed for this case, as shown in Figs. 11 and 12. The lower smoothness of the geometry results in half an order degradation in the convergence rate for the L_2 norm of the explicit residual estimator. It seems that the geometry smoothness affects only the residual error indicator. Its influence on the other error estimators is very small.

The asymptotic behavior of the estimators in L_1 norm for nozzle $\mathcal{D}_1(x)$ is presented in Fig. 13. The effectivity index of the error equation estimator is much lower than the others. This can be seen more clearly by plotting the error distributions for the grid of 321 points, as shown in Fig. 14, where the error based on Richardson extrapolation agrees well with the true error, whereas all others are quite far from it. Surprisingly, if one scales the errors of the residual and reconstruction estimators by the same constants used in the preceding supersonic case ($c_1 = 0.1$ and $c_2 = 0.12$, respectively), $|\mathrm{err}_{\mathrm{rect}}|$ agrees very well with $|\mathrm{err}_{\mathrm{eeq}}|$, as shown in Fig. 15, and the magnitude of $|\mathrm{err}_{\mathrm{rsd}}|$ is also much closer to that of $|\mathrm{err}_{\mathrm{eeq}}|$. The behavior of the three estimators is similar to that observed in the supersonic case, as shown in Fig. 7. For subsonic flow, one observes different error distributions for the true error and that obtained by solving the error equations. This nonnegligible discrepancy between the curves

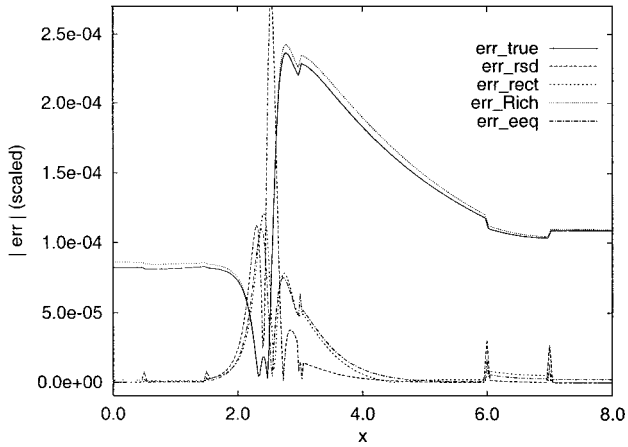

Fig. 15 Subsonic flow: scaled error distributions.

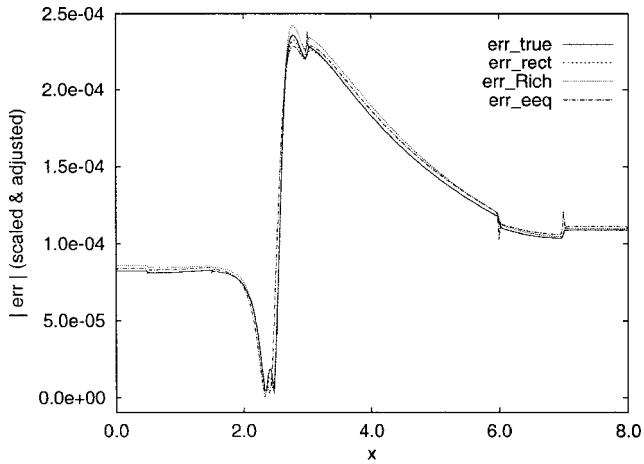

Fig. 16 Subsonic flow: scaled and adjusted error distributions.

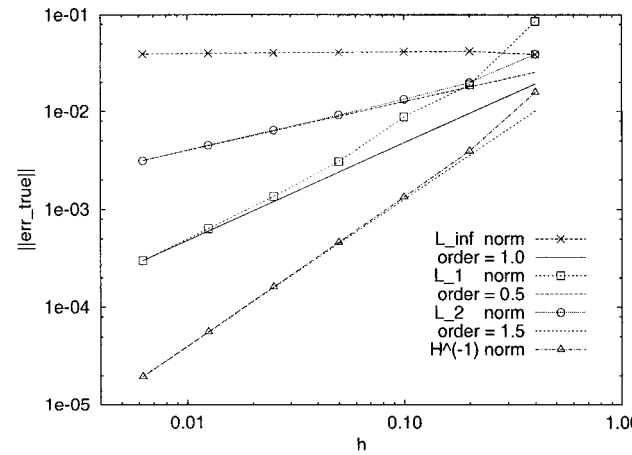

Fig. 17 Transonic flow: true momentum error in different norms.

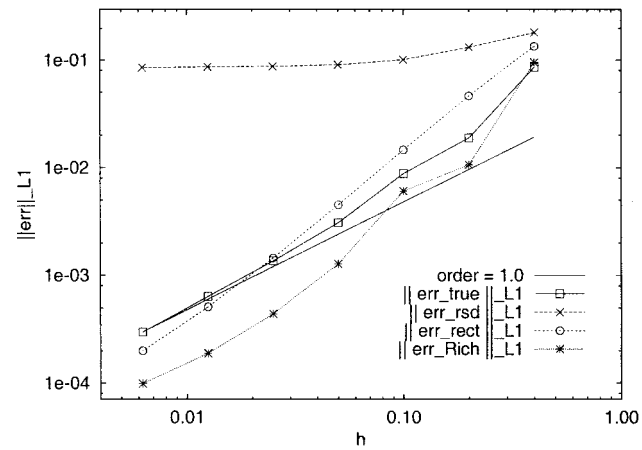

Fig. 18 Transonic flow: estimated momentum errors in L_1 norm.

may lead to completely different grids if the estimators were used to guide the grid adaptation.

The question now is, what causes these differences for supersonic and subsonic cases? It seems that the differences are mainly caused by differences in the treatment of subsonic and supersonic boundary conditions. On the one hand, for the supersonic case, all properties are set at the inlet point using the inlet Mach number and isentropic relations. This state is then propagated downstream. This implies that the inlet fluxes are exact. The total mass, momentum, and energy are well conserved downstream. On the other hand, for the subsonic case, the flow is determined by the back pressure at the outlet. A pressure wave is propagated upstream to the inlet, which generally causes a loss of accuracy. Differences result between the exact inlet pressure and its numerical approximation. Other inlet properties are evaluated based on this pressure and propagated downstream to the outlet. The outlet temperature and velocity are extrapolated from the upstream information. Even though the conservation scheme performs well, the inlet fluxes are not exact. Finally, note that extrapolation at the boundary points produces no significant errors because the geometries have constant area and fluid properties near boundaries.

The difference between the computed and exact mass fluxes at the inlet is about $e_f = f - f_h = -2.6E-4$ (where $f = \mathcal{D}\rho u$), which is actually very small. However, such a small difference can cause significant discrepancies in the error distributions of momentum. If we compensate for the inlet flux error e_f by adjusting the momentum error as follows:

$$e_{\text{new}}(x) = [e_{\text{old}}(x)\mathcal{D}(x) + e_f]/\mathcal{D}(x)$$

then the adjusted error distributions for the reconstruction and error equation estimates change their shapes significantly to come very close to the true error, as shown on Fig. 16. After this adjustment, excellent agreement is obtained for these error estimators.

Transonic Case

The last test is for a transonic nozzle with a shock downstream of the throat. The shock is located at $x = 5.2$ when the back pressure is set to $p = 0.75$. The inlet pressure is extrapolated from the first cell, and other properties are computed from isentropic relations. At the outlet, the velocity and the temperature are extrapolated.

The true momentum errors in L_∞, L_1, L_2, and H^{-1} norms are plotted in Fig. 17. This time, all four norms show different rates of convergence. The L_∞ norm does not converge. This is to be expected because there are jumps in all variables across the shock. The L_1 and L_2 norms show a convergence rate of 1 and 0.5, respectively, indicating that the accuracy of the scheme is first order in the L_1 norm and only of a half-order in the L_2 norm. This performance has been observed in previous work for two-dimensional problems.[18] Also, the H^{-1} norm has a convergence rate of 1.5. It seems that only the results measured in the L_1 norm agrees with the statement that the accuracy of a monotone upwind scheme is of first-order accuracy across a shock no matter which type of reconstruction is used to achieve higher-order accuracy.

For this transonic case, the error equation approach did not converge to a steady-state. Hence, we skip this error estimation for the present analysis. More detailed analysis about its steady-state performance will be presented in future work. Figures 18 and 19 compares the estimated errors in L_1 and L_2 norms for the three remaining error estimators. It is evident that the residual estimator does not converge in both norms and that the L_2 norm diverges with a rate of $\mathcal{O}(h^{-1/2})$, which agrees with the statement given in Refs. 14 and 15. In this case, the weak norm $\|h \cdot \text{err}_{\text{rsd}}\|_{L_2}$ has the same convergence rate as $\|\text{err}_{\text{exact}}\|_{L_2}$, but the error control theory given by Süli and Houston[17] seems too conservative. In the analysis given by Süli and Houston, the weak norm is used to control the true error in H^{-1} norm, with the result that the effectivity index tends to infinity $[\mathcal{O}(h)]$ for this test case. The reconstruction estimator

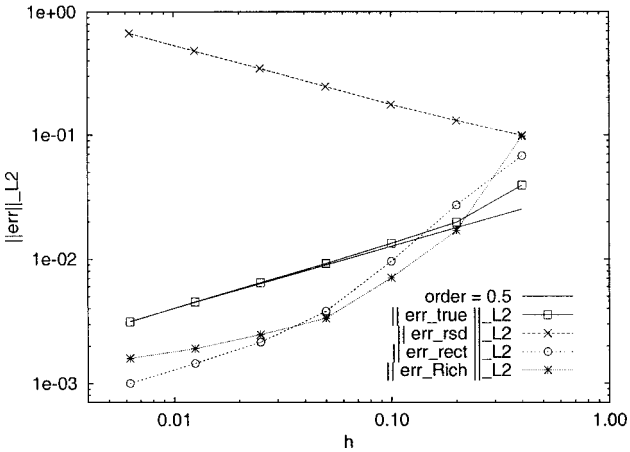

Fig. 19 Transonic flow: estimated momentum errors in L_2 norm.

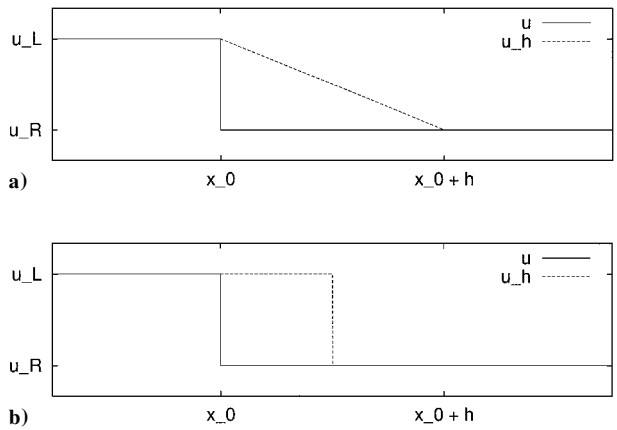

Fig. 20 Different solution reconstructions.

$\|\text{err}_{\text{rect}}\|$ exhibits a difference of one in the rates measured in L_1 and L_2 norms (about 1.5 for L_1 and 0.5 for L_2). This is mainly due to the derivatives across the shock. The Richardson extrapolation error $\|\text{err}_{\text{Rich}}\|$ behaves as if it has no asymptotic limit (no straight line for fine meshes). Its estimated convergence rates from Eq. (12) using the grids with 161, 321, and 641 points are about $\alpha_1 = 1.53$ and $\alpha_2 = 0.44$ with respect to the L_1 and L_2 norms. Because the Richardson estimator does not produce a straight line in Figs. 18 and 19 (the slope still changes), the convergence rates are likely erroneous when a shock is present. The value of α_2 seems close to the value found for the exact error, and the α_1 is about one-half an order higher. However, if one compares the slope between the last two points, α_1 is very close to one.

To verify the half-order difference between the L_1 and L_2 norms, the following analysis may be helpful. For the present case, the shock is always located at one node point $x_0 = 5.2$. To simplify the analysis, we assume that the total error is only due to the approximation error in the cell $K = [x_0, x_0 + h]$. If a traditional linear variation over K is used as in the finite element method (Fig. 20a), the error $e = u - u_h$ is given by

$$e = \begin{cases} 0, & x \le x_0 \\ (u_L - u_R)[(x_0 + h) - x]/h, & x_0 < x \le x_0 + h \\ 0, & x_0 + h < x \end{cases}$$

(with $u_L > u_R$) and represents the jump in variable u at x_0. Thus, the L_1 and L_2 norms of the error are

$$\|e\|_{L_1(\Omega)} = \|e\|_{L_1(K)} = [(u_L - u_R)/2]h$$

$$\|e\|_{L_2(\Omega)} = \|e\|_{L_2(K)} = \left[(u_L - u_R)/\sqrt{3}\right]h^{\frac{1}{2}}$$

For a finite volume method, reconstructions are computed in cells $[x_0 - h/2, x_0 + h/2]$ and $[x_0 + h/2, x_0 + 3h/2]$ (Fig. 20b). The error is then

$$e = \begin{cases} 0, & x \le x_0 \\ (u_L - u_R), & x_0 < x \le x_0 + h/2 \\ 0, & x_0 + h/2 < x \end{cases}$$

and the L_1 and L_2 norms of the error are

$$\|e\|_{L_1(\Omega)} = \|e\|_{L_1(K)} = [(u_L - u_R)/2]h$$

$$\|e\|_{L_2(\Omega)} = \|e\|_{L_2(K)} = \left[(u_L - u_R)/\sqrt{2}\right]h^{\frac{1}{2}}$$

In both cases, the errors in the L_1 and L_2 norms always exhibit a half-order difference with L_1 being of first-order and L_2 being of half-order accurate. This is exactly the situation for the transonic case with a shock. Away from the shock, the errors behaves just like in the supersonic and subsonic cases and are nearly second-order accurate. This is shown in Figs. 21 and 22 obtained by excluding the five neighboring points close to the shock when evaluating the global errors. This time, the convergence rates estimated from Eq. (12) are $\alpha_1 = 1.91$ and $\alpha_2 = 1.97$ in the L_1 and L_2 norms, respectively. Note that, for some cases, the error occurring at the shock may be transported downstream, as discussed in Ref. 19.

The asymptotic behavior of two error estimators based on reconstruction and Richardson extrapolation in the L_1 norm are presented in Fig. 23. The effectivity index of the residual error estimate tends to infinity. The error distributions for the grid of 321 points using the same scaling constants of $c_1 = 0.1$ and $c_2 = 0.12$ for residual and reconstruction errors are compared with true error and the estimates from Richardson extrapolation in Fig. 24. The adjusted profile for the reconstruction estimator with $e_f = -4.2E-5$ is compared to other distributions in Fig. 25. Away from the shock, the three error

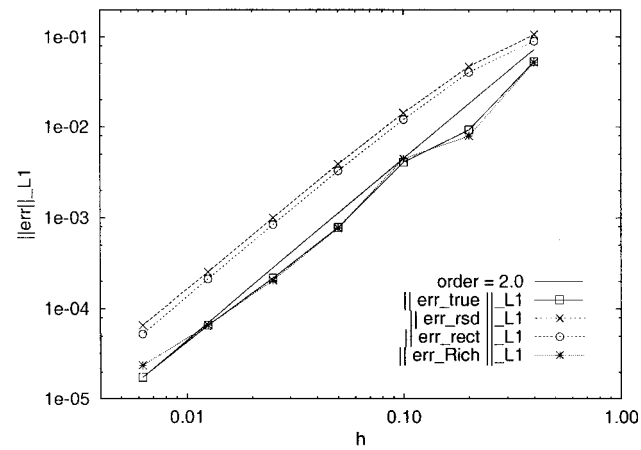

Fig. 21 Transonic flow: estimated errors excluding shock in L_1 norm.

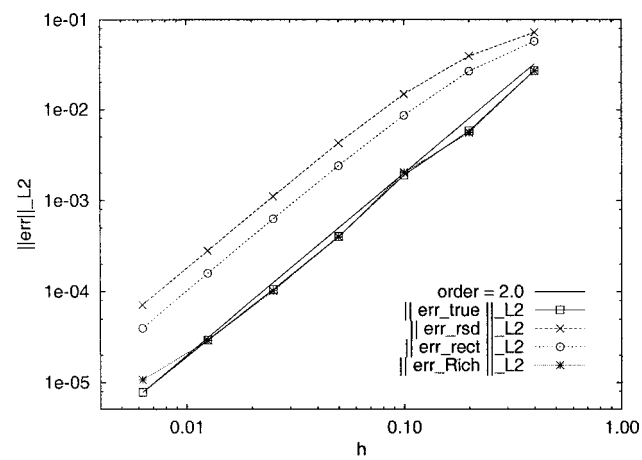

Fig. 22 Transonic flow: estimated errors excluding shock in L_2 norm.

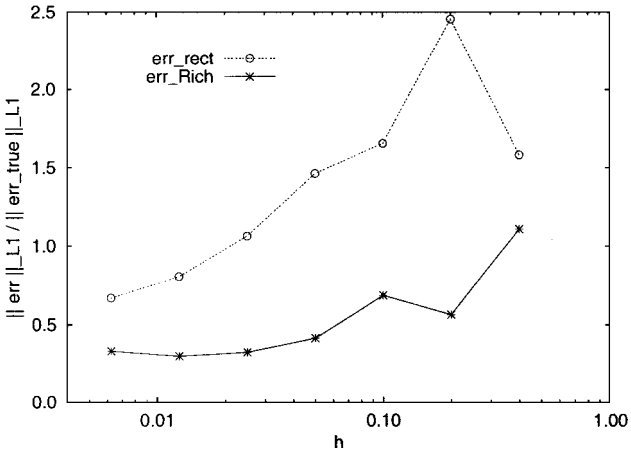

Fig. 23 Transonic flow: effectivity index of estimators in L_1 norm.

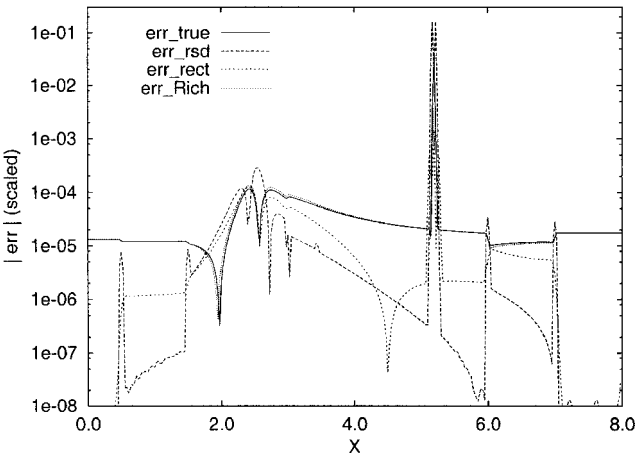

Fig. 24 Transonic flow: scaled error distributions.

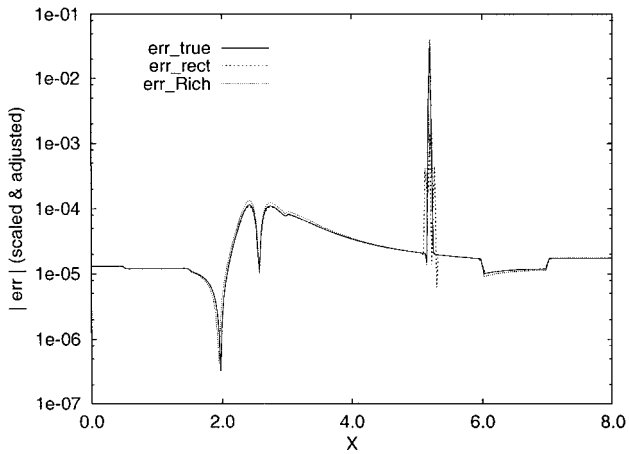

Fig. 25 Transonic flow: scaled and adjusted error distributions.

profiles agree almost perfectly. Even across the shock, the errors are detected well enough for grid adaptation.

Conclusions

From the present tests on quasi-one-dimensional problems, one can see that both the L_1 and L_2 norms of the errors yield second-order convergence rates for flows without shock. For flows with shocks, the L_2 norm yields only half an order of convergence rate, whereas the L_1 norm is of first-order convergence rate, which does agree with the accepted statement. Also, the L_1 norm is less sensitive to the smoothness of the geometry. It seems that the L_1 norm of the error estimators will probably be more reliable than the L_2 norm for grid adaptation and error control.

The weak norm in H^{-1} was proposed by Süli and Houston[17] for the flow with shocks. However, as demonstrated here, the use of a residual in a weak norm to control the true error in H^{-1} norm may not be as effective as one would expect because the effectivity index approaches infinity. For flows without shocks, its effectivity index tends to a nonunit constant. However, the stronger norms in L_1 and L_2 are much easier to compute and behave in the same way. Thus, there seems to be little need for the weak norm in H^{-1} in regions of smooth flow.

In all test cases, the estimated error using Richardson extrapolation agrees very well with the true error. The convergence rate is almost asymptotically exact except in the vicinity of a shock. This is because the theory, based on the Taylor series expansion, is not valid across discontinuities.

Error estimators based on solution reconstruction provide very good results with the use of the same scaling factor for all test cases. This does not mean such scaling constants are universal, but it may indicate that they may not differ much for different problems and numerical methods.

The error equation approach is expected to predict the transported errors for hyperbolic equations.[4,10] The reconstruction approach is based only on local variations of the solution and is expected to provide the local errors only. Surprisingly, these two approaches can yield very accurate error estimations when the upstream boundary condition in momentum is specified accurately, such as in the supersonic test case. However, for subsonic or transonic cases, the upstream boundary condition in momentum will be affected by the back pressure and its propagation upstream. This will lead to inaccurate error estimates. It can hardly be accurate again. For these test cases, compensation on the momentum can be implemented, and very good agreement can be achieved. Such adjustments are not practical for realistic problems. It is done here as a means to identify the error source. The control of such error sources is not obvious because no error estimators can predict this type of transport error. Finally, the error equation approach is more expensive and less robust than the reconstruction. Further studies are required.

Also note that the effectivity index of the rms value of the error based on reconstruction [see Eq. (11)] tends to infinity asymptotically for all test cases, indicating that it cannot be used to control the true error effectively. Nevertheless, it has been used quite successfully in grid adaptation for two-dimensional problems with shocks or expansion waves.[7] Its effectivity might be further improved by choosing a norm yielding asymptotic exactness of the error to guide mesh adaptation. Similar verifications for two-dimensional test cases are needed to assess the performance of using the rms to measure estimated local errors.

Acknowledgments

The financial support provided by the Natural Science and Engineering Research Council of Canada, the Fonds pour la Formation des Chercheurs et l'Aide à la Recherche of Québec, Bombardier Aerospace, and Air Force Office of Scientific Research Grant F49620-96-1-0329 is gratefully acknowledged.

References

[1] Johnson, C., and Szepessy, A., "Adaptive Finite Element Methods for Conservation Laws Based on A Posteriori Estimates," *Communications in Pure and Applied Mathematics*, Vol. 48, 1995, pp. 199–243.

[2] Süli, E., "A Posteriori Error Analysis and Adaptivity for Finite Element Approximations of Hyperbolic Problems," Computing Lab., TR 97/21, Oxford Univ., Oxford, Dec. 1997.

[3] Sonar, T., and Süli, E., "A Dual Graph-Norm Refinement Indicator for Finite Volume Approximations of the Euler Equations," *Numerische Mathematik*, Vol. 78, No. 4, 1998, pp. 619–658.

[4] Zhang, X. D., Trépanier, J.-Y., and Camarero, R., "A Posteriori Error Estimation Method for Finite-Volume Solutions of Hyperbolic Conservation Laws," *Computer Methods in Applied Mechanics and Engineering*, Vol. 185, No. 1, 2000, pp. 1–19.

[5] Palmério, B., and Dervieux, A., "2D and 3D Unstructured Mesh Adaption Relying on Physical Analogy," *Proceedings of the 2nd International Conference on Numerical Grid Generation in CFD*, Pineridge, Swansea, Wales, U.K., 1988, pp. 178–185.

[6] Reggio, M., Trépanier, J., Zhang, H., and Camarero, R., "Numerical Simulation of the Gas Flow in a Circuit-Breaker," *International Journal for Numerical Methods in Engineering*, Vol. 34, 1992, pp. 607–618.

[7]Peraire, J., Vahdati, M., Morgan, K., and Zienkiewicz, O., "Adaptive Remeshing for Compressible Flow Computations," *Journal of Computational Physics*, Vol. 72, 1987, pp. 449–466.

[8]Paillère, H., Powell, K., and De Zeeuw, D., "A Wave-Model-Based Refinement Criterion for Adaptive-Grid Computations of Compressible Flows," AIAA Paper 92-0322, 1992.

[9]Roache, P., "Perspective: A Method for Uniform Reporting of Grid Refinement Studies," *Journal of Fluid Engineering*, Vol. 116, No. 3, 1994, pp. 405–413.

[10]Houston, P., and Süli, E., "A Posteriori Error Indicators for Hyperbolic Problems," Computing Lab., TR 98/14, Oxford Univ., Oxford, 1998; also invited Lecture International Computational Fluid Dynamics Conf., Oxford, April 1998.

[11]Ciarlet, P., *The Finite Element Method for Elliptic Problems*, North-Holland, Amsterdam, 1978, Chap. 3.

[12]Morton, K., and Süli, E., "A Posteriori and A Priori Error Analysis of Finite Volume Methods," *Mathematics of Finite Elements and Applications*, edited by J. R. Whiteman, Wiley, New York, 1994, Chap. 18.

[13]Babuška, I., and Rheinboldt, W., "Error Estimates for Adaptive Finite Element Computations," *SIAM Journal on Numerical Analysis*, Vol. 15, No. 4, 1978, pp. 736–754.

[14]Sonar, T., "Strong and Weak Norm Refinement Indicators Based on the Finite Element Residual for Compressible Flow Computations," *Impact of Computing in Science and Engineering*, Vol. 5, 1993, pp. 111–127.

[15]Mackenzie, J., Sonar, T., and Süli, E., "Adaptive Finite Volume Methods for Hyperbolic Problems," *Mathematics of Finite Elements and Applications*, edited by J. R. Whiteman, Wiley, New York, 1994, Chap. 19.

[16]Sonar, T., Hannemann, V., and Hempel, D., "Dynamic Adaptivity and Residual Control in Unsteady Compressible Flow Computation," *Mathematical and Computer Modelling*, Vol. 20, No. 10/11, 1994, pp. 201–213.

[17]Süli, E., and Houston, P., "Finite Element Methods for Hyperbolic Problems: A Posteriori Error Analysis and Adaptivity," Computing Lab., TR 96/09, Oxford Univ., Oxford, May 1996.

[18]Ilinca, C., Zhang, X. D., Trépanier, J.-Y., and Camarero, R., "A Comparison of Three Error Estimation Techniques for Finite-Volume Solutions of Compressible Flows," *Computer Methods in Applied Mechanics and Engineering*, Vol. 189, No. 4, 2000, pp. 1247–1275.

[19]Roache, P., *Verification and Validation in Computational Science and Engineering*, Hermosa, Albuquerque, NM, 1998, Chap. 5.

[20]Aftosmis, M., Gaitonde, D., and Tavares, T., "Accuracy, Stability, and Monotonicity of Various Reconstruction Algorithms for Unstructured Meshes," AIAA Paper 94-0415, Jan. 1994.

[21]Zhang, X. D., Trépanier, J.-Y., and Camarero, R., "An A Posteriori Error Estimation Method Based on an Error Equation," *Proceedings of the AIAA 13th Computational Fluid Dynamics Conference*, AIAA, Reston, VA, 1997, pp. 383–397.

[22]White, F. M., *Fluid Mechanics*, 3rd ed., McGraw–Hill, New York, 1994, Chap. 9.

[23]Roe, P., "Characteristic-Based Schemes for the Euler Equations," *Annual Review of Fluid Mechanics*, Vol. 18, 1986, pp. 337–365.

[24]Zhu, J., "A Posteriori Error Estimation—The Relationship Between Different Procedures," *Computer Methods in Applied Mechanics and Engineering*, Vol. 150, No. 1–4, 1997, pp. 411–422.

[25]Babuška, I., and Rodriguez, R., "The Problem of the Selection of an A Postertiori Error Indicator Based on Smoothening Techniques," *International Journal for Numerical Methods in Engineering*, Vol. 36, No. 4, 1993, pp. 539–567.

[26]Zhang, X. D., Ilinca, C., Labbé, P., Trépanier, J.-Y., and Camarero, R., "On the Use of Residual Based Mesh Adaptive Strategies," *7th CFD Conference of Canada (CFD99)*, edited by J. Militzer, Dalhousie Univ., Halifax, NS, Canada, 1999, pp. 3-39–44.

J. Kallinderis
Associate Editor